Design of Electrically Small, Huygens Dipole Antenna with Quad-Polarization Diversity

Ming-Chun Tang, Zhentian Wu
College of Communication Engineering
Chongqing University
Chongqing, 400044, China
tangmingchun@cqu.edu.cn

Richard W. Ziolkowski
Global Big Data Technologies Centre
University of Technology Sydney
Ultimo NSW 2007, Australia
Richard.Ziolkowski@uts.adu.au

***Abstract* — The design of an electrically small, low-profile, Huygens dipole antenna with four reconfigurable polarization states is presented. This very compact design incorporates both electric and magnetic near-field resonant parasitic (NFRP) elements and a reconfigurable driven element. Reconfigurability is achieved with only six PIN diodes. By manipulating their ON/OFF states, this antenna dynamically achieves four polarization states which include two orthogonal linear (LP) and two circular polarization (LHCP and RHCP) states. The simulated values demonstrate that it is electrically small (*ka* = 0.944) and low profile (0.0449 λ_0) at 1.5 GHz.**

***Index Terms*—Electrically small antennas, low-profile antennas, Huygens dipole antennas, near-field resonant parasitic elements, polarization-reconfigurable antennas.**

I. Introduction

Electrically small antennas (ESAs) with high-directivity have received increasing attention in recent years. They provide significant advantages for many space-limited wireless platforms associated, for example, with long-distance and point-to-point communication systems [1]. To date, various methods for achieving higher directivity in small antenna systems have been widely considered. These include loading the radiating elements with electromagnetic band gap (EBG) structures [2], artificial magnetic conductors (AMC) [3], Quasi-Yagi designs [4-5], Huygens sources [6], and non-Foster elements [7]. The use of NFRP technologies to realize Huygens dipole ESAs has been researched and studied in recent years because these antennas can achieve high directivity and broadside radiation without significantly increasing their size and profile. We have recently developed several electrically small, NFRP, Huygens dipole antennas. These include, for example, linearly polarized and three-dimensional structures [8], multi-layered structures [9], and non-Foster designs [10].

However, it is expected that Huygens source ESAs could be even more useful if they were versatile. For instance, antennas with polarization reconfigurability have many advantages. These include mitigating polarization mismatch, improving system capacity, reducing channel interference, and realizing multiple transmission channels for frequency reuse [11]. Therefore, it would be highly desirable to enable polarization reconfigurability in an electrically small Huygens dipole antenna. Such a polarization diverse ESA would be suitable for many modern compact wireless applications [12].

A four-state, reconfigurable Huygens source antenna is reported in this paper. The antenna configuration is described in Section II. The simulated results are given in Section III. Finally, some conclusions are drawn in Section IV.

II. Reconfigurable Huygens Dipole ESA Design

A. Configuration

Fig. 1 illustrates the configuration of the polarization-reconfigurable Huygens source ESA. As shown in Fig. 1, the antenna consists of three substrate layers which are labeled as Layer_1, Layer_2 and Layer_3, respectively. All of these substrates are Taconic TLY-5. All these layers have the same radius, R1 = 30.0 mm. However, each of them has a different thickness: h1 = h2 = 0.25 mm, and h3 = 1.58 mm.

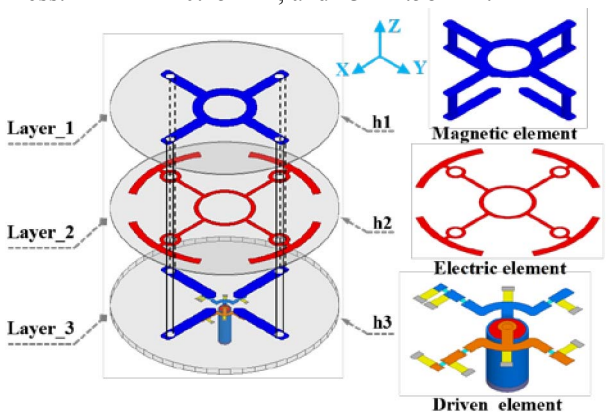

Figure 1. Geometry of the polarization-reconfigurable Huygens dipole ESA.

The magnetic element consists of two intersecting, orthogonally-oriented capacitively loaded loops (CLLs) whose sizes are the same, which has been extensively utilized [13]. One is oriented along the x-axis, and the other is along the y-axis. The upper face of the magnetic element is cross-shaped with a copper ring in the center and is located on the upper surface of Layer_1. Similarly, the electric element consists of two Egyptian axe dipoles (EADs) printed on the upper surface of Layer_2, each having the same size. One is oriented along the *x*-axis, and the other is along the *y*-axis. It

also has a copper ring in its center. The coax-driven element lies on the bottom surface of Layer_3.

B. Reconfigurable Driven Element Design

In order to realize the polarization reconfigurability amongst the two LP and two CP modes, a reconfigurable driven element was developed. Its configuration is highlighted in orange and blue in Fig. 2. There are eight additional rectangular copper patches (gray) distributed on the lower surface of Layer_3. As shown in Fig. 2, the Coilcraft inductors are installed between these patches and the driven element strips to block any RF signal from entering into the dc bias network. Each patch is used as the connection point for the dc feeder lines required to control the states of the diodes [14].

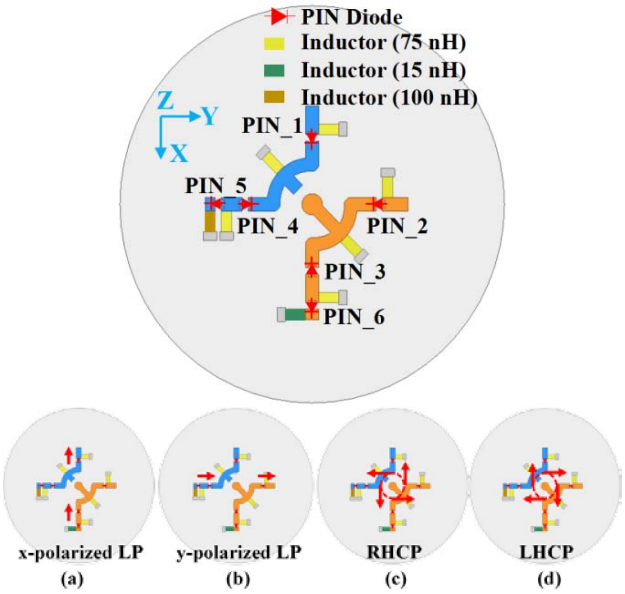

Figure 2. The locations of the six PIN diodes and the associated RF blocking inductors on the driven element. The current directions for each of the four polarization states are indicated by the red arrows in the bottom row of subplots. (a) *x*-polarized LP. (b) *y*-polarized LP. (c) RHCP. (d) LHCP.

Six M/A-COM MA4GP907 PIN diodes were incorporated into this driven element. For an easy description of their ON and OFF states, we have denoted these diodes as PIN_1 - PIN_6 and show their location in Fig. 2. According to the manufacturers datasheet, each diode acts as a 4 ohm resistor in its ON state and as a 0.025 pF capacitor in its OFF state. The control of the radiated polarization with the PIN diode states is summarized in Table I.

TABLE I
THE PIN DIODE STATES TO ATTAIN THE FOUR POLARIZATION STATES

Category	*State*	*PIN_1*	*PIN_2*	*PIN_3*	*PIN_4*	*PIN_5*	*PIN_6*
Fig.2 (a)	*X-LP*	*ON*	*OFF*	*ON*	*OFF*	*OFF*	*OFF*
Fig.2 (b)	*Y-LP*	*OFF*	*ON*	*OFF*	*ON*	*OFF*	*OFF*
Fig.2 (c)	*RHCP*	*ON*	*ON*	*ON*	*ON*	*ON*	*OFF*
Fig.2 (d)	*LHCP*	*ON*	*ON*	*ON*	*ON*	*OFF*	*ON*

III. SIMULATED RESULTS OF THE POLARIZATION-RECONFIGURABLE HUYGENS DIPOLEE ESA

The simulated S-parameters for the two LP and the two CP polarization states are presented in Fig. 3.

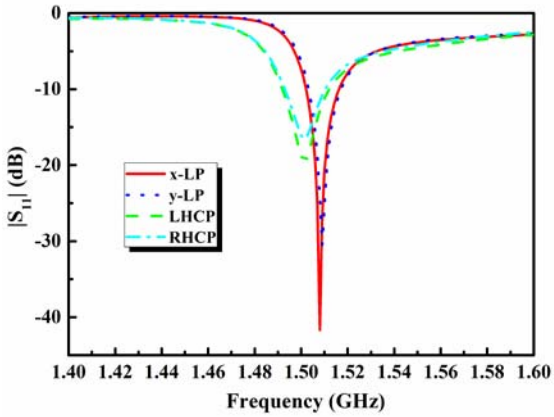

Figure 3. Simulated $|S_{11}|$ values of the four polarization states of the reconfigurable Huygens dipole ESA as functions of the source frequency.

The simulated resonance frequency of the *x*- (*y*-) LP state is 1.508 (1.509) GHz, where $|S_{11}|_{min}$ = -41.6 (-30.0) dB. The simulated -10-dB bandwidths are 1.503-1.516 GHz (13 MHz, 0.86% fractional bandwidth, FBW) and 1.504-1.517 GHz (13 MHz, FBW = 0.86%) for the *x*- and *y*-LP states, respectively. Thus, the simulated overlapped operating bandwidth for the two LP states is 12 MHz, covering 1.504–1.516 GHz (FBW = 0.86%). Similarly, the simulated resonance frequency of the LHCP (RHCP) state is 1.501 (1.501) GHz, where $|S_{11}|_{min}$ = -19.5 (-16.5) dB. The simulated -10-dB bandwidths are 1.492-1.512 GHz (20 MHz, FBW = 1.33%) and 1.493-1.51 GHz (17 MHz, FBW = 1.13%) for these LHCP and RHCP states, respectively. Thus, the simulated overlapped operating bandwidth for the LHCP and RHCP states is 17 MHz, covering 1.493–1.51 GHz (FBW = 1.13%).

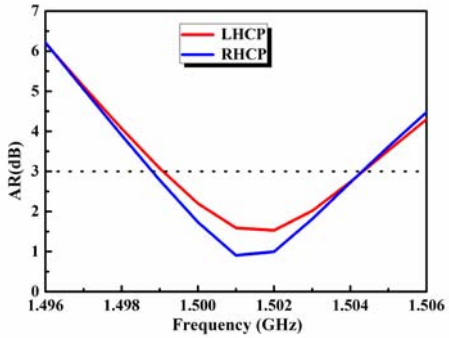

Figure 4. Simulated AR values when the polarization-reconfigurable Huygens dipole ESA is radiating its LHCP and RHCP states.

The axial ratio (AR) values of the two CP states are plotted in Fig. 4 as functions of the source frequency. The simulated 3-dB AR bandwidths are 1.4991-1.5043 GHz (5.2 MHz, FBW = 0.34%) and 1.4988-1.5043 GHz (5.5 MHz, FBW = 0.36%) for the LHCP and RHCP states, respectively. The simulated overlapped operating 3-dB AR bandwidth is 1.4991-1.5043 GHz (5.2 MHz, FBW = 0.34%).

Fig. 5 presents the simulated normalized realized gain patterns when the antenna radiates each of its four polarization states. The main-beam direction for each of these states is clearly broadside, oriented along the +z-axis.

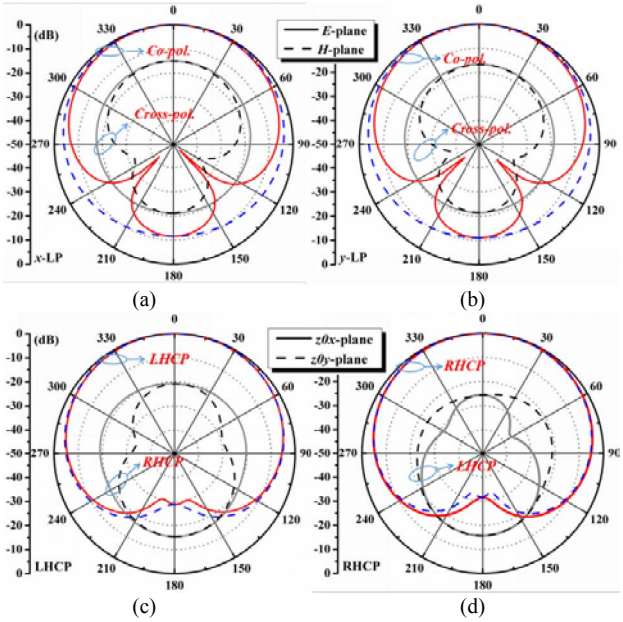

Figure 5. Simulated 2D realized gain patterns for the four polarization states at their resonance frequencies. (a) *x*-LP. (b) *y*-LP. (c) LHCP. (d) RHCP.

The simulated normalized realized gain patterns of the *x*- (*y*-) LP states are shown in Figs. 5(a) and 5(b), respectively. In the *x*- (*y*-) LP state, the simulated peak realized gain, FTBR, and radiation efficiency values are ~3.51 (3.54 dBi), ~11.2 (11 dB), and ~77.9 (78.9%), respectively. The simulated half-power beamwidth is from -61.5° to 62.9° (from -60.5° to 62.3°) in the E-plane and from -76.6° to 76.5° (from -77.4° to 77.7°) in the H-plane. The cross-polarization levels in the broadside direction are below -15 dB for both LP states, indicating their high polarization purity.

The simulated normalized realized gain patterns of the LHCP (RHCP) states are shown in Figs. 5(c) and 5(d), respectively. In the LHCP (RHCP) state, the simulated peak realized gain, FTBR, and radiation efficiency values are ~3.13 (2.99 dBi), ~15.2 (15.5 dB), and ~71.3% (69.8%), respectively. The simulated half-power beamwidth is from -68.1° to 68.3° (from -68.6° to 70.6°) in the *z0x*-plane and from -71.1° to 68.7° (from -68.4° to 68.6°) in the *z0y*-plane.

IV. Conclusion

A polarization-reconfigurable Huygens dipole ESA was presented. Rather than altering previously successful Huygens dipole NFRP elements, the reported multi-functional configuration was achieved through the development of a novel, reconfigurable driven element implemented with six PIN diodes. By manipulating their ON/OFF states, it was demonstrated that this ESA is capable of dynamically achieving four different polarization states, i.e., two LP and two CP states, which are radiated with their maximum gain in the broadside direction. The multi-functionality attained with this polarization-reconfigurable approach could be extended to many other types of reconfigurable antennas. The realized system has a number of potential applications to the next generation wireless systems, e.g., to narrowband MIMO communication systems [15] and narrowband WiFi connections [16].

References

[1] W. Hong, Y. Yamada, and N. Michishita, "Low profile small normal mode helical antenna achieving long communication distance," *in Proc. Int. Workshop Antenna Technol. (iWAT 2008)*, Chiba, Japan, Mar. 2008, pp. 167–170.

[2] P. Jin and R. W. Ziolkowski, "High-directivity, electrically small, low-profile near-field resonant parasitic antennas," *IEEE Antennas Wireless Propag. Lett.*, vol. 11, pp. 305-309, 2012.

[3] A. Erentok, P. L. Luljak, and R. W. Ziolkowski, "Characterization of a volumetric metamaterial realization of an artificial magnetic conductor for antenna applications," *IEEE Trans. Antennas Propag.*, vol. 53, no. 1, pp. 160-172, Jan. 2005.

[4] M.-C. Tang, T. Shi, and R. W. Ziolkowski, "Flexible efficient quasi-Yagi printed uniplanar antenna," *IEEE Trans. Antennas Propag.*, vol. 63, no. 12, pp. 5343-5350, Dec. 2015.

[5] M.-C. Tang, R. W. Ziolkowski, S. Xiao, and M. Li, "A high-directivity, wideband, efficient, electrically small antenna system," *IEEE Trans. Antennas Propag.*, vol. 62, no. 12, pp. 6541 - 6547, Dec. 2014.

[6] P. Jin and R. W. Ziolkowski, "Metamaterial-inspired, electrically small Huygens sources," *IEEE Antennas Wireless Propag. Lett.*, vol. 9, pp. 501-505, 2010.

[7] M.-C. Tang, N. Zhu, and R. W. Ziolkowski, "Augmenting a modified Egyptian axe dipole antenna with non-Foster elements to enlarge its directivity bandwidth," *IEEE Antennas Wireless Propag. Lett.*, vol. 12, pp. 421-424, 2013.

[8] M.-C. Tang, H. Wang, and R. W. Ziolkowski, "Design and testing of simple, electrically small, low-profile, Huygens source antennas with broadside radiation performance," *IEEE Trans. Antennas Propag.*, vol.64, no. 11, pp. 4607-4617, Nov. 2016.

[9] M.-C. Tang, T. Shi, and R. W. Ziolkowski, "A study of 28 GHz, planar, multi-layered, electrically small, broadside radiating, Huygens source antennas," *IEEE Trans. Antennas Propag.*, in the Special Issue on "Antennas and Propagation Aspects of 5G Communications", vol. 65, no. 12, pp. 6345-6354, Dec. 2017.

[10] M.-C. Tang, T. Shi, and R. W. Ziolkowski, "Electrically small, broadside radiating Huygens source antenna augmented with internal non-Foster elements to increase its bandwidth," *IEEE Antennas Wirel. Propag. Lett.*, vol.16, pp. 712-715, 2017.

[11] F. Wu and K. M. Luk, "A reconfigurable magneto-electric dipole antenna using bent cross-dipole feed for polarization diversity," *IEEE Antennas Wireless Propag. Lett.*, vol. 16, pp. 412–415, 2017.

[12] C. G. Christodoulou, Y. Tawk, S. A. Lane, and S. R. Erwin, "Reconfigurable antennas for wireless and space applications," *Proc. IEEE*, vol. 100, no. 7, pp. 2250–2261, Jul. 2012.

[13] M.-C. Tang, H. Wang, T. Deng, and R. W. Ziolkowski, "Compact planar ultra-wideband antennas with continuously tunable, independent band-notched filters," *IEEE Trans. Antennas Propag.*,vol.64, no. 8, pp. 3292-3301, Aug. 2016.

[14] Y. Shang, S. Xiao, M.-C. Tang, Y.-Y. Bai, and B. Wang, "RCS reduction of microstrip patch antenna using PIN diodes," *IET Microwaves, Antennas & Propagation*, vol. 6, Iss. 6, pp. 670 - 679, Jun. 2012.

[15] A. Grau, J. Romeu, M.-J. Lee, S. Blanch, L. Jofre, and F. De Flaviis, "A dual-linearly-polarized MEMS-reconfigurable antenna for narrowband MIMO communication systems," *IEEE Trans. Antennas Propag.*, vol. 58, no. 1, pp. 4–17, Jan. 2010.

[16] Z. N. Chen, X. M. Qing, T. S. P. See, and W. K. Toh, "Antennas for WiFi connectivity," *Proc. IEEE*, vol. 100, no. 7, pp. 2322–2329, Jul. 2012.